Golden Research Thoughts
Vol -2 , ISSUE –10, April.2013
ISSN:- 2231-5063

Available online at www.aygrt.net

ORIGINAL ARTICLE

AC AND DC ELECTRICAL PROPERTIES OF NANOPARTICLE SIZE ALUMINUM SUBSTITUTED COBALT FERRITE

R.A.BUGAD[b] , T.R.MANE[b] , C.S.PAWAR[a] AND B.R.KARCHE[a]

[a] Shankarrao Mohite Mahavidyalaya,Akluj.Dist: Solapur (M.S)

[b]Research scholars, JJT University, Jhunjhunu, Rajasthan .

ABSTRACT

Nano-particle size polycrystalline aluminum substituted cobalt ferrite samples $CoFe_{2-2y}Al_{2y}O_4$ (where y = 0.0, 0.05, 0.15 and 0.25) have been prepared by standard ceramic technique. The lattice constants of the phases are evaluated from x-ray diffraction data. The effects of Al^{3+} on both AC and DC Electrical properties are studied. DC Electrical resistivity is found to increase with increase of aluminum content. Activation energies in ferromagnetic region are found very less than that of paramagnetic region. The SEM micrograph reveals that an average grain size increases with aluminum content. The dielectric constant ε', complex permittivity ε" and dielectric loss tangent (tanδ) measured at room temperature as a function of the frequency. The effect of Al^{3+} ion substitution of cobalt ferrite on the AC electrical resistivity and dielectric properties in frequency range 20 Hz to 1MHz. were studied. The data revealed that ε' and tanδ increased as the Al^{3+} ion increased , due to the increase in the number of vacancies at the iron site.

KEY WORDS:-

Co-Al Ferrites, Polycrystalline, , Inverse cubic spinel, Dielectrics , activation energy, resistivity, SEM, XRD,

INTRODUCTION:-

Spinel ferrites are an important class of compounds having large variety of electronic, magnetic and catalytic properties as they possess high resistivity and negligible eddy current losses. Cobalt ferrite is a partially inverse spinel with formula $(Co_yFe_{2-2y})^A$ [$Co_{2-2y}Fe_{2+2y}]^B$ O_4 where A and B are the tetrahedral and octahedral sites respectively (1-3). Vaingankar et.al (4)

has reported that cobalt is 74% inverse spinel. Degree of inversion is found to vary with heat treatment and quenching (5). The cation distribution may also differ at surface and nonsurface atoms (6).

Nano ferrites material has application in making high density information storage (7), cores of audio frequency and high frequency transformer coils, magneto optical displays, electromagnetic wave absorption (8). Nanoferrites are at present very promising material in technological applications and drug delivery (9). Polycrystalline ferrites, which have applications ranging from microwave frequencies to radio frequencies range are very good dielectric materials. The very low conductivity of these materials is suitable for microwave applications. The dielectric properties of ferrites depend upon the preparation techniques. Knowledge of the dielectric properties is also important from the view point of applications at high frequencies. (10).

Cobalt ferrite is having high coercive force field, mechanical hardness and chemical stability is magnetic recording, magneto-optical recording and electronic devices (7). Magnetic properties of nanoparticles find wide technological applications such as high density recording, magnetic refrigeration, Ferro-fluids, Spintronics etc.(11). Several researchers have reported on Cd, Cr, Mn, Ti, Zn, Gd, and Nd. Substituted cobalt ferrite (12-14). The present study is mainly concerned with experimental results of dielectric properties of $CoFe_{2-2y}Al_{2y}O_4$ nanoparticles. The aim of this work is to study the effect of Al -ions on the behaviour of dielectric properties at different frequencies. In the present work; we reported the influence of composition on resistivity and microstructure of $CoFe_{2-2y}Al_{2y}O_4$ ferrite.

EXPERIMENTAL PROCEDURE:-

The ferrites with general chemical formula $CoFe_{2-2y}Al_{2y}O_4$ (where y = 0.0, 0.05, 0.15 and 0.25) were prepared by the standard ceramic technique using AR grade cobalt oxide, Ferric oxide and aluminum oxide. The compositional weights of powders were mixed physically and blended in agate mortar in acetone medium. The final sintering process was carried at 1000^0C for 48 hours. The slow cooled samples were heated at rate of 80^0C per hour. The pellets and toroids were formed by using respective steel die. The pressure was applied of 10 tones / square inch by hydraulic pressure gauge. The formation of the cubic spinel structure of the samples prepared is confirmed by X- ray diffraction analysis and Infrared absorption spectroscopic investigations. D.C. resistivity was measured by a four probe method on compressed and sintered pellets. Silver paste was applied on both of the flat surfaces of the pellet for good electric contacts. A low but constant voltage was applied across the sample and current through the sample was measured as a function of temperature. The activation energy was calculated from the variation in resistivity with temperature using the formula

$$\rho = \rho_0 \exp(\Delta E/KT) \text{ ----------(1)}$$

Dielectric measurements were carried out at room temperature using 4192A impedance over a wide frequency range from 20 Hz up to 1 MHz. The dielectric constant (ε') , dielectric loss (ε'') and loss tangent (tanδ) were calculated using the formulas

$$\varepsilon' = \frac{cd}{\varepsilon_0 A} \qquad \text{----------(2)}$$

$$\varepsilon'' = \tan\delta\varepsilon' \qquad \text{----------(3)}$$

$$\tan\delta = \frac{\varepsilon'}{\varepsilon''} \qquad \text{----------(4)}$$

Where c is the capacitance, d the thickness of the sample, A the cross-section area, ε_0 the free space permittivity.

$$\rho_{ac} = R_P A / d \text{ ---------- (5)}$$

where R_P = Parallel resistance
Micrographs were taken using JEOL scanning electron microscope.

RESULT AND DISCUSSION:-

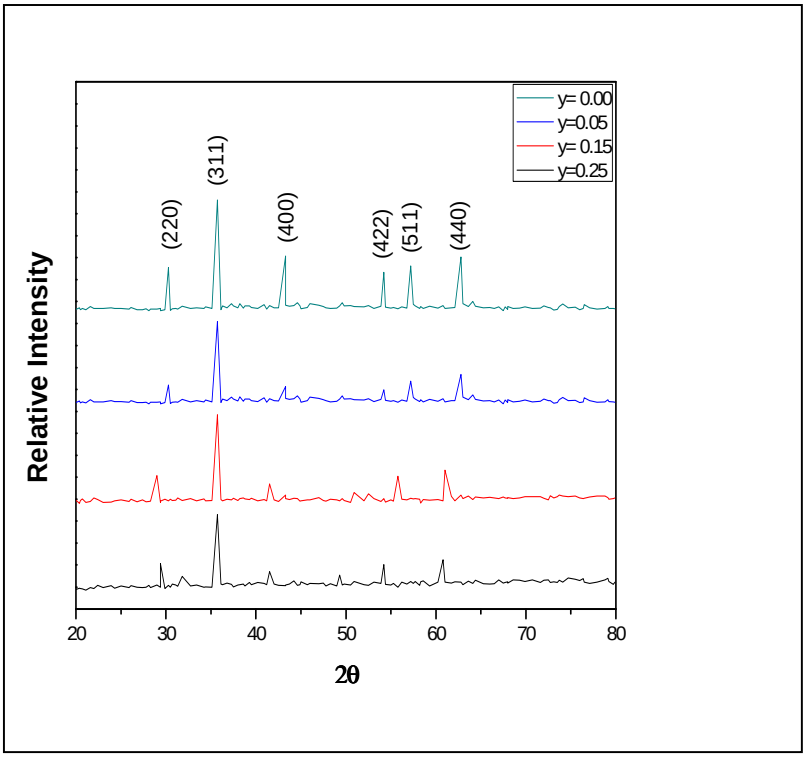

Fig.1 XRD of $CoFe_{2-2y}Al_{2y}O_4$ ferrite system.

Powder XRD (Fig.1) of the ferrite samples reveals the single-phase cubic spinel structure, as well-defined reflections are observed without any ambiguity. The average particle size 'D' was determined from line broadening (311) reflection using the Debye Scherer formula discussed elsewhere (30). Calculations of lattice constant , physical density, X-ray density, porosity, site radii and ionic bond lengths on both sites were calculated by using formulae discussed elsewhere (31) and presented in (Table 1). Lattice constant 'a' decreases with addition of Al^{3+} in the host lattice of cobalt cubic spinel ferrite.

The calculated particle size is in good agreement with previous reports (28). Addition of Al^{3+} occupies on B site which replaces Fe^{3+} ions from B- site to A- site and hence lattice constant and particle size goes on decreases. It is authenticated cause that Al^{3+}(0.55 A^0) ion is smaller in size than Fe^{3+} (0.67A^0) ion. Similar type of reports is found in the literature (29) for aluminum substituted Nickel ferrite.

Table 1 X-ray characterization data of Ferrite $CoFe_{2-2y}Al_{2y}O_4$ system

Composition y	Lattice constant In A.U.	Ionic Radii. Tetrahedral (R_A) in A.U.	Ionic Radii Octahedral (R_B) in A.U.	Ionic Bond length Tetrahedral (A-O) in A.U.	Ionic Bond length Octahedral (B-O) in A.U.
y =0.00	8.370	0.552	0.694	1.902	2.045
y=0.05	8.360	0.547	0.690	1.897	2.040
y=0.15	8.345	0.543	0.686	1.893	2.036
y=0.25	8.323	0.539	0.682	1.889	2.031

SEM

The SEM micrographs of Aluminum substituted Cobalt ferrite sample $CoFe_{2-2y}Al_{2y}O_4$ (where y = 0.0, 0.05, 0.15 and 0.25) were obtained in reflection mode. The measurement of grain size is counted by counting the number of grain boundaries intersected by a known measured length from the magnification. By drawing random such line and repeating same procedure average grain size is calculated [20]. The particle size is found in the nano scale.The SEM micrographs are presented in figure 2. Close inspection of the micrographs shows that the average grain size decreases with increasing substitution of doping concentration of Al^{3+} in cobalt ferrite with increase in porosity. From the Table.2 it is seen that X-ray density, physical

density, linearly decreases with increase in Al^{3+} content. Porosity is found to increase with Al^{3+} content. The present investigation shows close agreement with previous reports (21).

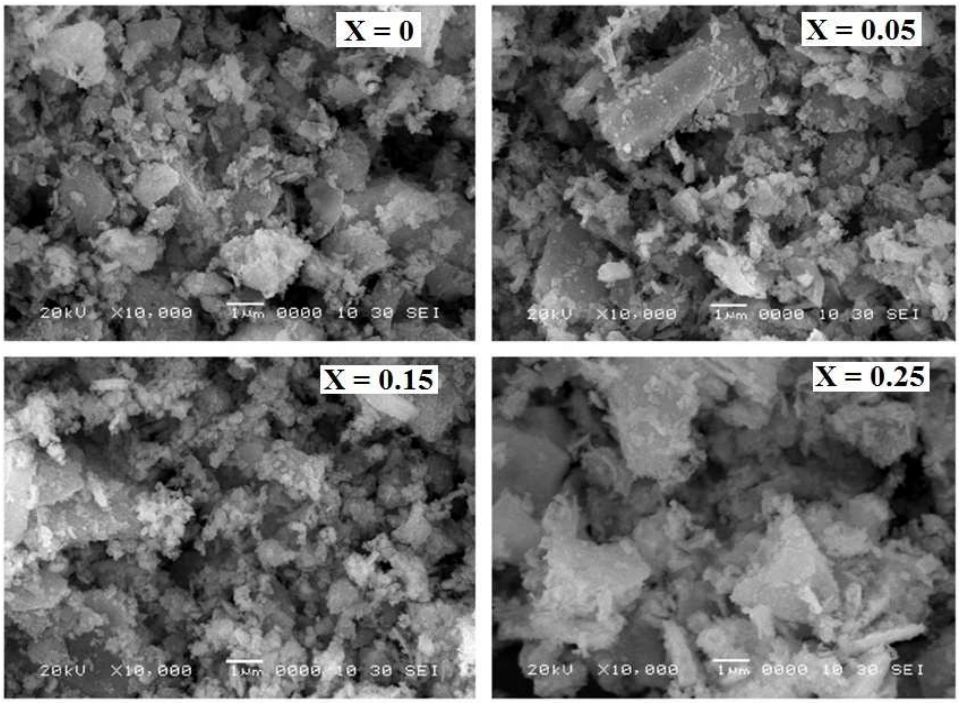

Figure 2. SEM micrographs of $CoFe_{2-2y}Al_{2y}O_4$ (where y = 0.0, 0.05, 0.15 and 0.25)

Table 2 Microstructural data of $CoFe_{2-2y}Al_{2y}O_4$ Ferrite system

Composition y	X-ray density dx (gm/cm3)	physical density d_B (gm/cm3)	Porosity	Particle size t (nm)
y =0.00	5.305	3.610	0.3195	161.76
y=0.05	5.273	3.561	0.3247	145.76
y=0.15	5.169	3.161	0.3265	104.1
y=0.25	5.078	3.106	0.3883	99.12

D.C electrical resistivity

D.C electrical resistivity for all the samples was measured as a function of temperature is shown in figure1. DC electrical resistivity for all the samples was measured by four probe method.

From Fig.3 it is observed that DC electrical resistivity of all the samples show almost a linear decreasing behaviour with increasing temperature. According to (15), Ferrite

structurally forms cubic close packed oxygen lattice with the cations fit into the octahedral(B) and tetrahedral (A) sites. It is observed that DC electrical resistivity increases with increasing concentration of Al^{3+} ions. Conduction in ferrite can be explained on the basis of hopping mechanism. It is well known that Al^{3+} occupy octahedral site B, while Co^{2+} and Fe^{3+} ions occupy A and B sites (16). More, it is known that the conduction mechanism in ferrite occurs mainly through the hopping between $Fe^{2+} \leftrightarrow Fe^{3+}$ in the B- sıtes (32). Thus , the deficient of Fe^{2+} ions with increasing Al^{3+} concentrations gives further reason for the increase of the DC electrical resistivity. The Fe^{3+} ions at the A- sites contribute little to conduction due to larger distance between them (17).

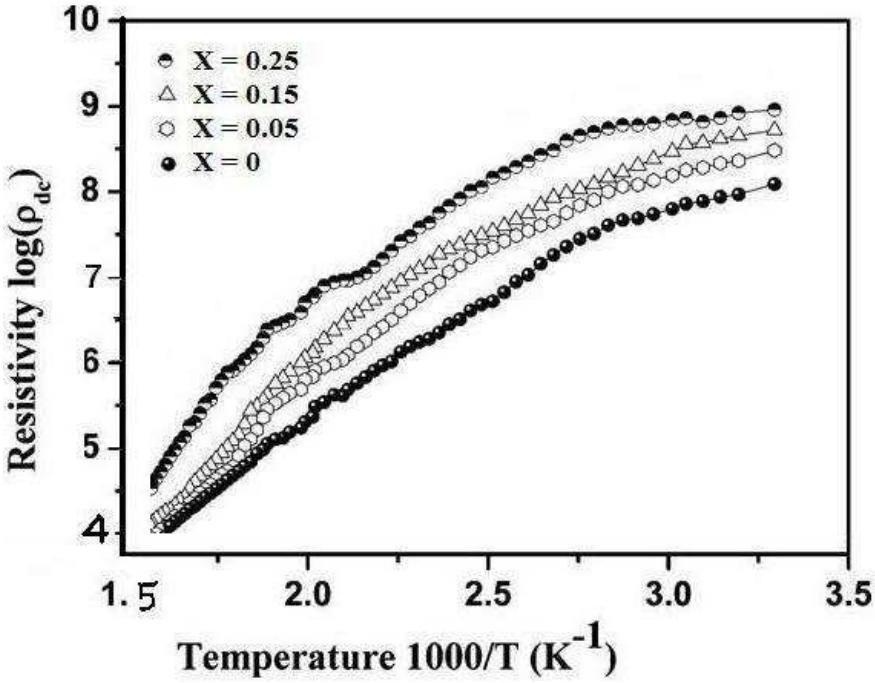

Figure 3. Variation of DC resistivity with temperature.

Table3. Activation energy, Curie Temp. and dc resistivity of $CoFe_{2-2y}Al_{2y}O_4$ ferrite system.

Composition y	Activation Energy (eV)		Curie Temp. in ^0K
	Ferri-region	Para-region	
y =0.00	0. 2694	0.4149	765
y=0.05	0.3230	0.4391	730
y=0.15	0.2570	0.4705	701
y=0.25	0.3123	0.5724	669

The change in slope is markedly observed in all the samples, such change is either due to Curie temperature (18) or due to change in conduction. This indicates the semiconducting nature of ferrrites. The variation in resistivity with temperature is given by using the formula

$$\rho = \rho_0 \exp(\Delta E/KT) \quad \text{----------(6)}$$

Where ΔE = Activation energy, K = Boltzmann constant & T = Absolute temperature.

For composition y = 0.0, 0.05, 0.15 and 0.25, the variation of log ρ with 1/T shows only one discontinuity in resistivity at curie temperature. The change in the slope of resistivity at Curie temperature corresponds to change in the activation energy (ΔE). Komer and klisuhin have attributed the change of activation energy to magnetic transformation from ferrimagnetic to paramagnetic state. (19).

The activation energies in both ferri and paramagnetic region of the composition are determined from the slope of respective lines. Activation energies in ferrimagnetic region are found very less than that of a paramagnetic region as shown in Table.3

DIELECTRIC CONSTANT BEHAVIOUR

The dielectric constant was determined using equation (2) . The dielectric properties of ferrite nanoparticles are influenced mainly by the synthesis technique, grain size, cation distribution etc (33). Fig.4. shows the variation of Dielectric constant (ε') as a function of frequency from 20 Hz to 1 MHz Samples having high D.C. electrical resistivity acquire low values of dielectric constant and vice versa (Gul and Maqsood 2008). Generally, dielectric constant, ε', decreases with increasing frequency. The increase of the dielectric constant (ε') with Al ions substitution can be explained on the basis of mechanism of polarization process in ferrites, which is similar to that of conduction process.

The addition of Al ions increase the iron on B – sites, which is mainly responsible for both space charge polarization and hopping exchange between the localized states. Therefore, increasing of Al ions content causes increase in the polarization, which is accomplished by a increase of dielectric constant, ε', of the composition. Koops (1951) proposed that the effect of grain boundaries is predominant at lower frequencies. The thinner the grain boundary, the value of dielectric constant is higher. It is seen that the value of the dielectric constant is very high at low frequencies and decreases with increasing frequency, and then at higher frequency they become almost constant. At higher frequencies the electron exchange between ferrous and ferric ions cannot follow the alternating field. At lower frequencies grain boundary are more effective

than grain electrical conduction. The higher value of dielectric constant at low frequency is due to to voids, dislocations and other defects (22).

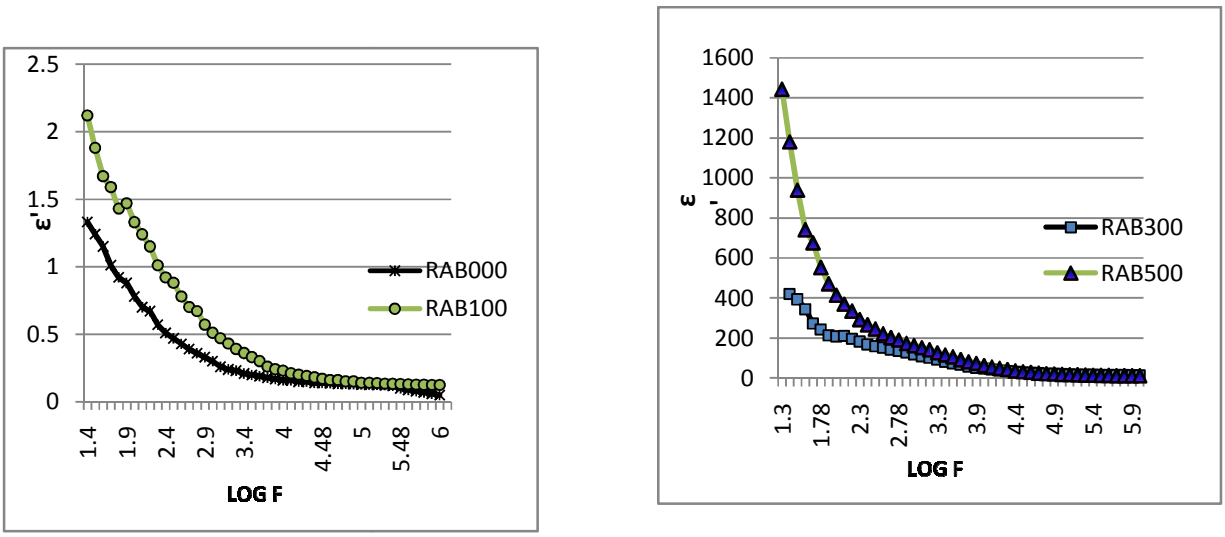

Figure 4. Dielectric constant (ε') for the samples $Co\ Fe_{2-2y}Al_{2y}O_4$ ferrites

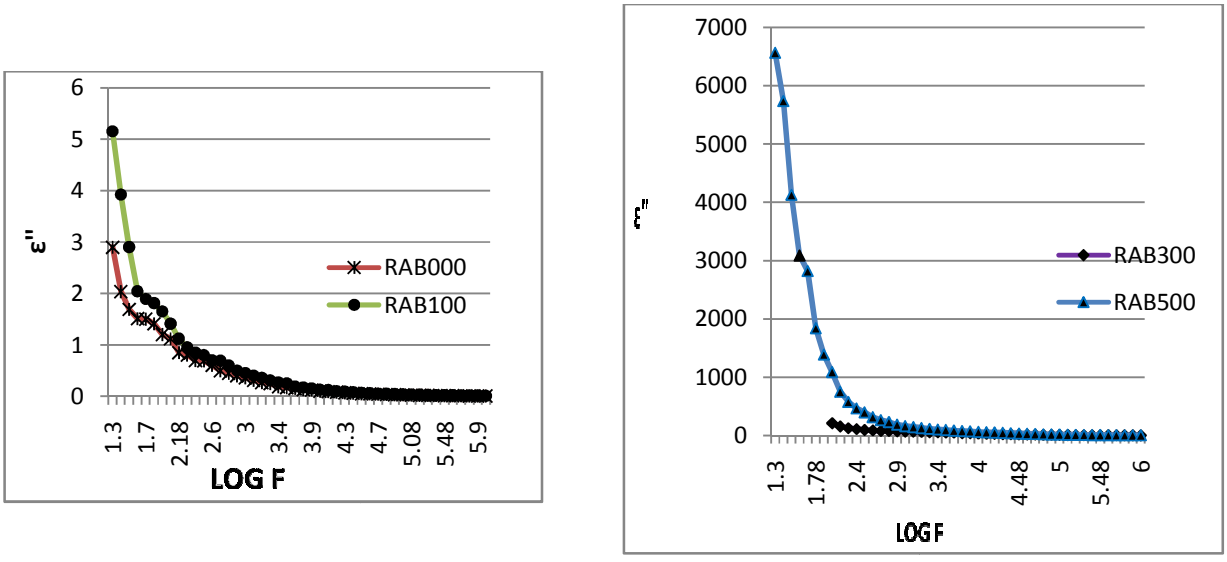

Figure 5. Complex permittivity (ε'') for the samples $Co\ Fe_{2-2y}Al_{2y}O_4$ ferrites

The imaginary part of the dielectric constant (ε'') is a measure of the absorption of energy by the dielectric from the alternating field. It is also called Complex permittivity. The dielectric loss factor ε'' was determined by using equation (3). Dielectric loss factor ε'' is an important part of

the total core loss in ferrites. Hence for low core loss, low dielectric losses are desirable. The dielectric loss factor ε'' as a function for all the composition is shown in figure 5. The dielectric loss factor profile is similar to those of the real part of dielectric constant. The increase in hoping electron result in a local displacement in the direction of the extent electric field causing an increase in electric polarization enhances dielectric loss factor. Hudson (23) has shown that, the dielectric losses in ferrite a generally reflected in the conductivity measurement, where the materials of highly conductivity shows high losses and vice versa.

Dielectric loss tangent (tan δ)

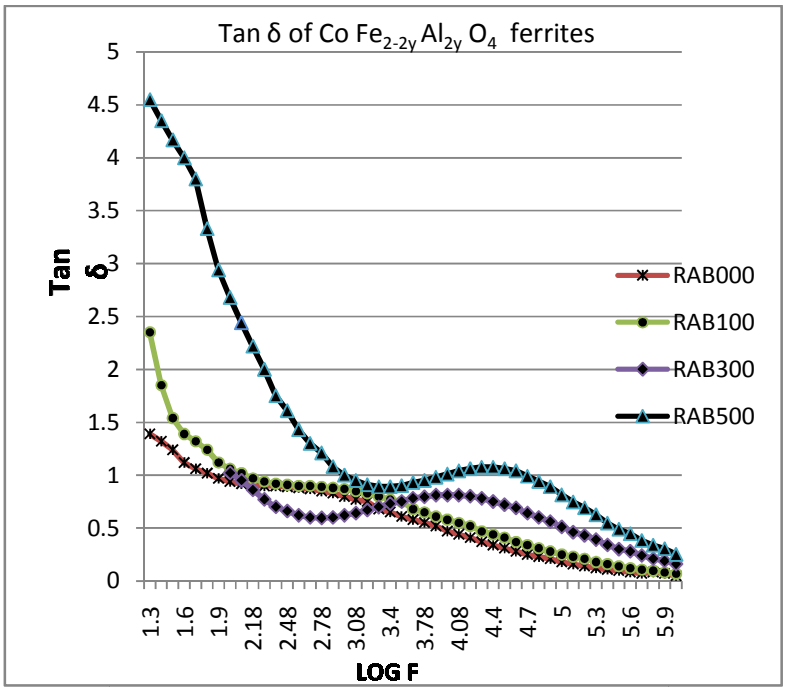

Figure 6. Dielectric loss tangent (tan δ) for the samples Co Fe_{2-2y} Al_{2y} O_4 ferrite

The dielectric loss tangent was determined using equation (4). Fig.6. Shows the variation of dielectric loss tangent tanδ at room temperature as a function of applied field frequency in the range 20 Hz to 1 MHz for all the samples of Co Fe_{2-2y} Al_{2y} O_4 ferrite. . It can be seen that dielectric loss tangent tanδ in each composition is found to decrease with increase in applied frequency. The decrease in tan δ takes place when the jumping rate of charge carriers lags behind the alternating electric field beyond a certain critical frequency. The change in dielectric loss tangent is greater at low frequencies and small at high frequencies for the all the samples. The decrease in dielectric loss tangent with change in the composition and frequency is in accordance with Koops phenomenological model (Koops 1951) (24). A small abnormal behavior was observed for all samples at lower frequencies. According to Rezlescu model the relaxation peak may be

due to the collective contribution of both p and n type carriers (25). The electron exchange between $Fe^{2+} \leftrightarrow Fe^{3+}$ and hole transfer between Co^{2+} and Co^{3+} in octahedral sites are responsible for such behavior. Thus both n and p type carriers take part in the conduction. Furthermore the jumping frequencies of localized charge carriers are almost equal to that of the applied A.C. electric field.

AC RESISTIVITY

Fig.7 illustrates the variation of AC resistivity as a function of applied field frequency in the range 20 Hz to 1 MHz for all the samples. It can be seen that, the AC resistivity with frequency is found to decrease with increase in applied frequency. According to (26), AC resistivity decreases with increase in applied frequency. The dispersion in the dielectric constant and AC resistivity is observed in low frequency region, which is analogues to the results predicted by Koop (27) that dielectric constant of ferrite material is inversely proportional to square root of AC resistivity of that material i.e. ε' .

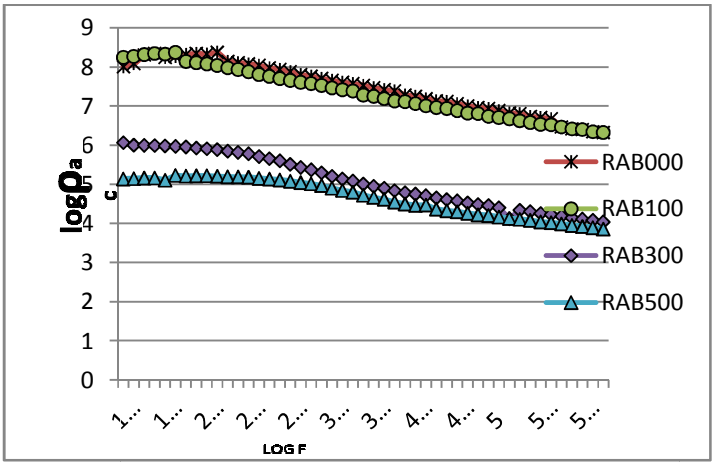

Figure 7. AC Resistivity for the samples $Co\ Fe_{2-2y}\ Al_{2y}\ O_4$ ferrites

CONCLUSION:-

Cobalt ferrite is partially inverse cubic spinel ferrite. Addition of Al^{3+} ions replaces Fe^{3+} on (B) site resulting in decrease of lattice constant, ionic radii and bond length. All prepared ferrite samples exhibit single domain to super paramagnetic transition. The electrical properties have been studied for all samples. The resistivity variation with temperature shows typical semiconductor characteristics. The decrease in resistivity with increasing temperature could be attributed to negative temperature coefficient of resistance of $CoFe_{2-2y}Al_{2y}O_4$. The decrease in the electrical resistivity at low temperature is attributed to the impurities, which reside at the grain boundaries. The micrographs showed that the average grain size decreases with increasing substitution of doping concentration of Al^{3+} in cobalt ferrite. Therefore it is concluded that aluminum content influences electrical conductivity and microstructure of cobalt ferrite. It is seen that the value of dielectric constant ε' and dielectric loss tangent ε" increases with addition of $Al3^{+}$ ions. Dielectric constant and complex permittivity decreases rapidly with increasing

frequency, and then reaches a constant value. Hence much lower dielectric constants obtained for the ferrites are used in the applications at high frequencies as microwave absorbers.

ACKNOWLEDGEMENT:-

One of the authors (R. A. Bugad) would like to thanks Dr. Sanjay Latte for valuable co-operation in case of SEM and DC resistivity characterization.

REFERENCES:-

1. K. Haneda and A. H. Morish, J .Appl. Phys. 63 (1988) 4285.
2. L. Zhavo et al ; Mat. Lett. 60 (2006) 1.
3. N. N. Greenwood and T. C. Gibb. Mossbauer spectroscopy.((Chapman and Hall Ltd., London.(1971) 261-66.
4. A. S. Vaingankar, S. A. Patil and Sahashrabudhye, Trans. Indian. Inst. metals 34, 5 (1981) 387.
5. Ohbayashik and Iida S. J., Phy. Soc. Japan 23 (1967) 776.
6. E. J. Choi et.al., J.Magn.Mater.262 (2003) L118.
7. R.F. Zolio, US patent 4,474(1984) 866 .
8. S.N. Dolia, Solid State Phenomena, 2011, 171 79-91.
9. Mytil Kahn and John Zhang 2001; Sousa et al 2005.
10. Raghavender and Jadhav 2009 ; Mater. Sci. ,. Vol. 32 .
11. P. C. Rajesh Varma et.al,J. Alloys.comp.453 (2008) 29.
12. M. L. Khan, Z. Jhon Zhang, Appl.Phys.Lett.78 (2001) 3651.
13. P. M. Vasambekar, C. B. Kolekar and A.S.Vaingankar; Mat.Chem.Phys.60 (1999)282.
14. J. F. Hochepied, M. P.Pileni, J.Phys.87 (2000) 2472.
15. A.Verma , O. P. Thakur, C. Prakash, T.C. Goel, R.G. Mendiratta, J. Mater.Sci. Eng.B,116 (2005) ,
16. A. A. Sattar, J.mater.Sci., 39 (2004) 451.
17. A.Verma , O. P. Thakur, C. Prakash, T.C. Goel, R.G. Mendiratta, J. Mater.Sci. Eng.B,116 (2005).
18. Ravinder, D. and B. Ravikumar, ” Mater.Sci. Lett., Vol. 15, 1605 – 1608, 1996.

19. Komar K. P. , Kliushin V. V. , Bull. Acad. Sci. USSR, 18 (1954) 403.
20. Karche B. R., Khasbardar B. V., and Vaingankar A. S., J. of Mag. And Mag. Mat., 168 (1997) 292
21. Certo J, Furtado C.S, Ferreira A.R, and Perdigao J.M, J. Mat. Sci.,30 (1995) 3248.
22. Sirdeshmukh. K. kumar, b. laxman, k. a. rama, g. sathaiah, bull Mater Sci.,21 (1998)219.
23. K.M. Jadhav, V.B. Kawade, et al , Physics B, 291 (2000) 379.
24. A.T. Raghvender and K.M. Jadhav D-2007 J. Mater. Sci.vol 32, 578
25. Rezlescu and Rezlescu 1974; Gul and Maqsood 2008.
26. Van Hipple A.R. , " Dielectric and Waves" , John Wiley and Co., New York., 1954.
27. Van Uitert L.G., Proc. IRE, 44 (1956) 1294.
28. A. T. Raghvendra, R. G. Kulkarni and K.M. Jadhav; Chinese J. of Phys.vol.48 No.4 (2010) 512-522.
29. T. Raghvendra et.al., magn. mater. 316 (2007) 1.
30. H. P. Klug, L. E. Alexander, X-ray diffraction procedure for polycrystalline and amorphous materials,(Willey N.Y 1997)637.
31. A. B. Gadkari, T. J. Shinde, P. N. Vasambekar, J. Mater Sci: Mater Electron 21 (2010) 96-103.
32. B.K.Bammannavar, B.K.Chougule,L.R.Naik and R.B.Pujar, J.Progress in lectromagnetic research letters, vol.4, 121-129 (2008).
33. A.T.Raghavender and K.M.Jadhav (2009) J.Bull Mater. Sci. Vol.32. No. 6, 575-578.